

Online state and parameter estimation in Dynamic Generalised Linear Models

Rui Vieira

School of Mathematics and Statistics
Newcastle University, UK
`r.vieira2@ncl.ac.uk`

Darren J. Wilkinson

School of Mathematics and Statistics
Newcastle University, UK
`darren.wilkinson@ncl.ac.uk`

Abstract

Inference for streaming time-series is tightly coupled with the problem of Bayesian on-line state and parameter inference. In this paper we will introduce Dynamic Generalised Linear Models, the class of models often chosen to model continuous and discrete time-series data. We will look at three different approaches which allow on-line estimation and analyse the results when applied to different real world datasets related to inference for streaming data. Sufficient statistics based methods delay known problems, such as particle impoverishment, especially when applied to long running time-series, while providing reasonable parameter estimations when compared to exact methods, such as Particle Marginal Metropolis-Hastings. State and observation forecasts will also be analysed as a performance metric. By benchmarking against a “gold standard” (off-line) method, we can better understand the performance of on-line methods in challenging real-world scenarios.

1 Introduction

With the modern ubiquity of large streaming datasets comes the requirement of robust real-time inference. A multitude of different data sources, such as Internet of Things (IoT) devices, server, network and sensor metrics all exhibiting particular patterns and observation types, also

increase the demand for flexible and computationally cheap solutions.

Some typical analyses performed on such streaming time-series are forecasting, anomaly detection and seasonal decomposition in order to perform statistically-based decisions typically under tight time constraints.

As standard off-line methods, such as Markov Chain Monte Carlo (MCMC), are not normally suitable when taking into account such constraints, we analyse in this paper alternatives such as Sequential Monte Carlo (SMC). Although SMC is well studied in the scientific literature and quite prevalent in academic research in the last decade, modern analytics platforms typically still resort to less powerful methods (such as moving averages). When coupled with Dynamic Generalised Linear Models (DGLMs), which allow us to specify complex, non-linear time-series patterns, this enables performing real-time Bayesian estimations in state-space models.

Inference on streaming time-series is tightly coupled with the problem of Bayesian on-line state and parameter inference. In this paper we will perform a comprehensive review of some well established methods for SMC for DGLMs applied to three distinct datasets. We will start by first introducing the DGLM, the class of state space models chosen for our data (Section 1.1).

We will then look in Section 2 at the fundamentals of SMC and in Section 3 we will look

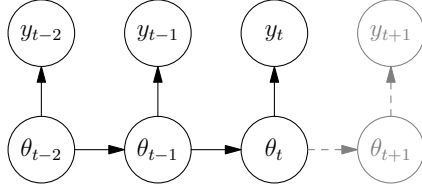


Figure 1.1: State-Space Model

at three algorithms which allow us to perform on-line estimation. Finally in Section 4 we will look at applications and analyse the results when applied to different real world datasets. We will also focus on topics which are directly relevant to the main application area which we approach, streaming time-series, such as the choice of resampler and the accumulation of Monte Carlo errors in long running series.

1.1 Dynamic Generalised Linear Models

To model the data we chose the Dynamic Generalised Linear Model (DGLM) [26], a specific instance of the more general class of State-Space Models (SSM), illustrated in Figure 1.1, where we have the following relations

$$y_t | \boldsymbol{\theta}_t, \Phi \sim f(y_t | \boldsymbol{\theta}_t, \Phi) \quad (1.1)$$

$$\boldsymbol{\theta}_t | \boldsymbol{\theta}_{t-1}, \Phi \sim g(\boldsymbol{\theta}_t | \boldsymbol{\theta}_{t-1}, \Phi). \quad (1.2)$$

Usually (1.1) is referred to as the *observation model* and (1.2) as the *system model*. We consider the discrete time case with $t \in \mathbb{N}$, the state vector $\boldsymbol{\theta}_t \in \mathbb{R}^m$ and Φ as the set of parameters for this model. The sequence of state vectors $\boldsymbol{\Theta}_t$ is a Markov Chain (conditional on Φ) with transition density g , such that

$$\boldsymbol{\Theta}_t | \{\boldsymbol{\Theta}_{t-1} = \boldsymbol{\theta}_{t-1}\} \sim g(\cdot | \boldsymbol{\theta}_{t-1})$$

and the sequence of observations $\mathcal{D}_t = \{y_1, \dots, y_t\}$ is the output of $\boldsymbol{\Theta}_t$ such that $Y_t | \{\boldsymbol{\Theta}_t = \boldsymbol{\theta}_t\} \sim f(\cdot | \boldsymbol{\theta}_t)$.

The second component, the *system model* (1.2), defined by the function $g : \mathbb{R}^m \mapsto \mathbb{R}^m$ can be non-linear and specifically

in DGLMs will be a linear Gaussian update of the form

$$\boldsymbol{\theta}_t | \boldsymbol{\theta}_{t-1}, \Phi \sim p(\boldsymbol{\theta}_t | \boldsymbol{\theta}_{t-1}, \Phi) \quad (1.3)$$

$$\stackrel{\text{DGLM}}{=} \mathcal{N}(\mathbf{G}_t \boldsymbol{\theta}_{t-1}, \mathbf{W}) \quad (1.4)$$

where the initial state is assumed to be distributed according to a normal prior, $\boldsymbol{\theta}_0 | \mathbf{m}_0, \mathbf{C}_0 \sim \mathcal{N}(\mathbf{m}_0, \mathbf{C}_0)$. In DGLMs the observation model, characterised by the density $f : \mathbb{R}^m \mapsto \mathbb{R}^n$, follows an exponential family distribution in the canonical form of (1.6)

$$y_t \sim p(y_t | \eta_t) \quad (1.5)$$

$$= \exp \left\{ \frac{z(y_t) \eta_t - b(\eta_t)}{a(\phi_t)} + c(y_t, \phi_t) \right\}. \quad (1.6)$$

In the literature η_t is usually called the *natural parameter* and ϕ_t the *dispersion parameter*. We consider $a(\cdot)$ to be twice differentiable in η_t .

We will consider throughout the case where $y_t \in \mathbb{R}$, the continuous univariate case or $y_t \in \mathbb{N}$, the discrete univariate case.

Furthermore, the state vector $\boldsymbol{\theta}_t$ is related to η_t by a link function $L(\cdot)$, such that

$$\eta_t = L(\mathbf{F}_t^T \boldsymbol{\theta}_t)$$

which will be dependent on the specific distribution used in (1.5).

The factors \mathbf{F}_t and \mathbf{G}_t are respectively the *observation* and *system matrices*. They allow us to specify the structure of our time series. These factors might represent a *locally constant model*, where the states will represent an underlying mean, a *locally linear model*, where the states represent a mean and a trend, or a purely seasonal model, where each component of the state will represent a seasonality component. A specific way of representing seasonality is the *reduced form Fourier seasonality*. Here, we represent cyclical components by a composition of harmonics. These matrices can vary in time but for the remainder of this text we will consider them static and known, that is $\mathbf{F}_t = \mathbf{F}$ and $\mathbf{G}_t = \mathbf{G}$.

It is clear from the above definitions that this class of models possesses Markovian properties,

that is, denoting the sequence of observations $y_{1:t-1}$ as \mathcal{D}_{t-1} :

$$p(\theta_t | \theta_{1:t-1}, \mathcal{D}_{t-1}) = p(\theta_t | \theta_{t-1}). \quad (1.7)$$

DGLMs are a flexible and elegant tool to model streaming data, since they can represent discrete and continuous data by appropriate selection of the observation model, as well as providing the means to express complex time-series behaviour by composing simpler ones. In the remainder of this paper we will refer to a specific DGLM by classifying it according to the observation model, as detailed below.

Normal DLM A special case of the DGLM is the Normal DLM where the observation model also consists of a normal distribution,

$$y_t | \theta_t, \Phi \sim \mathcal{N}(F^T \theta_t, V), \quad (1.8)$$

where the state model is (1.4). In this case, an analytical solution for the filtering problem exists, namely the Kalman filter (KF) [14]. However, Kalman filtering allows solely for state estimation and not, by itself, parameter estimation.

Poisson DLM The Poisson DLM is another instance of a DGLM, where the observation model follows a Poisson distribution

$$y_t | \lambda_t \sim \text{Po}(\lambda_t), \text{ where } \log(\lambda_t) = F^T \theta_t.$$

Binomial DLM In the presence of binary data the Binomial DLM can be used

$$y_t | \lambda_t \sim \text{Binom}(n, \lambda_t), \text{ where } \text{logit}(\lambda_t) = F^T \theta_t. \quad (1.9)$$

2 Sequential Monte Carlo

In order to perform inference in DGLMs, the main objective is to estimate the unobserved sequence of states $\theta_{0:t} = \{\theta_0, \dots, \theta_t\}$ and the parameter set $\Phi = \{\Phi_1, \dots, \Phi_n\}$ given the observed

data, $\mathcal{D}_t = \{y_1, \dots, y_t\}$. That is, we are trying to estimate the joint density

$$p(\theta_{0:t}, \Phi | \mathcal{D}_t) \quad (2.1)$$

We will first look at some methods to estimate the state vectors in an on-line fashion, that is estimating $\theta_{0:t}$ using \mathcal{D}_t with $t = 1, 2, 3, \dots$, while considering the parameters Φ known. These methods will provide the fundamental framework from which extensions can be used to simultaneously estimate state and parameters in Section 3.

2.1 State Estimation

Assuming the set of parameters Φ to be known, in DGLMs the problem of estimating the unobserved states $\theta_{0:n}$ can be expressed as

$$p(\theta_{0:t} | \mathcal{D}_t) = \frac{p(\theta_{0:t}, \mathcal{D}_t)}{p(\mathcal{D}_t)}, \quad (2.2)$$

where

$$p(\theta_{0:t}, \mathcal{D}_t) = p(\mathcal{D}_t | \theta_{0:t}) p(\theta_{0:t}), \quad (2.3)$$

$$p(\mathcal{D}_t) = \int p(\theta_{0:t}, \mathcal{D}_t) d\theta_{0:t}.$$

The Markovian nature of the DGLMs can, however, be exploited to provide a recursive formulation for the state estimation in (2.2). This is crucial in allowing on-line inference in DGLMs, since it provides us with a tool to perform computations for each time step t separately from the previous time steps. Considering $\mathcal{D}_{t-1} = y_{1:t-1}$, the state posterior can then be expressed as a recursive update:

$$p(\theta_{0:t} | \mathcal{D}_t) = p(\theta_{0:t-1} | \mathcal{D}_{t-1}) \frac{p(\theta_t | \theta_{t-1}) p(y_t | \theta_t)}{p(y_t | \mathcal{D}_{t-1})}$$

where $p(y_t | \mathcal{D}_{t-1})$ is a normalising constant. The joint posterior can then be expressed recursively as

$$p(\theta_{0:t}, \mathcal{D}_t) \propto p(\theta_{0:t-1}, \mathcal{D}_{t-1}) p(y_t | \theta_t) p(\theta_t | \theta_{t-1}) \quad (2.4)$$

However, in order to perform on-line state estimation, we need to perform the estimation as the observations appear, *i.e.* we need to estimate the *current state* (conditional on the observations). This is usually referred in the literature as *Bayesian filtering* and targets the state's marginal posterior

$$p(\boldsymbol{\theta}_t | \mathcal{D}_t). \quad (2.5)$$

The *filtering* method can be divided into two separate stages, the *prediction* and the *update* steps. In the prediction step we calculate the predictive state density given the observations up to time $t - 1$, this is

$$p(\boldsymbol{\theta}_t | \mathcal{D}_{t-1}) = \int p(\boldsymbol{\theta}_t | \boldsymbol{\theta}_{t-1}) p(\boldsymbol{\theta}_{t-1} | \mathcal{D}_{t-1}) d\boldsymbol{\theta}_{t-1}.$$

State estimation, also commonly referred as *filtering* aims at determining the density

$$p(\boldsymbol{\theta}_t | \mathcal{D}_t) = \frac{p(y_t | \boldsymbol{\theta}_t) p(\boldsymbol{\theta}_t | \mathcal{D}_{t-1})}{p(y_t | \mathcal{D}_{t-1})}. \quad (2.6)$$

2.2 Importance Sampling

In this context, state estimation can be viewed as the calculation of arbitrary expectations of the form

$$\bar{g} = \mathbb{E}[g(\boldsymbol{\theta}) | \mathcal{D}_t] = \int g(\boldsymbol{\theta}) p(\boldsymbol{\theta} | \mathcal{D}_t) d\boldsymbol{\theta} \quad (2.7)$$

Here, $g(\cdot)$ is an arbitrary function and $p(\boldsymbol{\theta} | \mathcal{D}_t)$ is the state's posterior probability density given the entirety of the data $\mathcal{D}_t = y_{1:t} = \{y_1, \dots, y_t\}$. This distribution may be highly complex and with high dimensionality. The problem with the integral in (2.7) is that typically we cannot solve it analytically. In such cases we can employ a Monte Carlo approximation by producing samples $s^{(i)}$ from a support distribution, with corresponding weights $w^{(i)}$, where $\sum_{i=1}^N w^{(i)} = 1$, such that

$$\sum_{i=1}^N g(s^{(i)}) w^{(i)} \simeq \int g(\boldsymbol{\theta}) p(\boldsymbol{\theta} | \mathcal{D}_t) d\boldsymbol{\theta}, \quad (2.8)$$

an approximation which will converge in probability when $N \rightarrow \infty$.

In the case of Importance Sampling (IS) we assume an *importance density* π , having a larger support than p , from which we can easily sample, that is

$$\boldsymbol{\theta}^{(i)} \sim \pi(\boldsymbol{\theta}_{0:n} | \mathcal{D}_t). \quad (2.9)$$

In this case, the weights will correspond to $w^{(i)} = A p(s^{(i)}) / \pi(s^{(i)})$ with $A^{-1} = \sum_{i=1}^N p(s^{(i)}) / \pi(s^{(i)})$ [4], accounting for the difference between the target and importance densities.

If we consider our target density $p(\boldsymbol{\theta})$ and our proposal draws $\boldsymbol{\theta}' \sim \pi(\boldsymbol{\theta})$, it follows that, starting from (2.7):

$$\bar{g} = \int g(\boldsymbol{\theta}) \tilde{W}(\boldsymbol{\theta}) \pi(\boldsymbol{\theta}) d\boldsymbol{\theta}$$

Here, $\tilde{W}(\boldsymbol{\theta})$ is the *unnormalised importance weight* and is given by

$$\tilde{W}(\boldsymbol{\theta}) = \frac{p(\boldsymbol{\theta})}{\pi(\boldsymbol{\theta})}. \quad (2.10)$$

Given (2.10), we can then approximate our expectation in (2.7) by

$$\begin{aligned} \bar{g} &\approx \frac{1}{N} \sum_{i=1}^N \frac{p(\boldsymbol{\theta}^{(i)} | \mathcal{D}_t)}{\pi(\boldsymbol{\theta}^{(i)} | \mathcal{D}_t)} g(\boldsymbol{\theta}^{(i)}) \\ &= \sum_{i=1}^N \tilde{w}^{(i)} g(\boldsymbol{\theta}^{(i)}) \end{aligned}$$

Here the weights are defined by

$$\tilde{w}^{(i)} = \frac{1}{N} \frac{p(\boldsymbol{\theta}^{(i)} | \mathcal{D}_t)}{\pi(\boldsymbol{\theta}^{(i)} | \mathcal{D}_t)}. \quad (2.11)$$

However, in this case we must be able to evaluate $p(\boldsymbol{\theta}^{(i)} | \mathcal{D}_t)$. Recalling the posterior density in (2.6) we can see that the denominator will not

be easily calculated. However if we write the expectation in (2.7) as

$$\mathbb{E}[g(\boldsymbol{\theta}_t) | \mathcal{D}_t] \approx \sum_{i=1}^N w_t^{(i)} g(\boldsymbol{\theta}_t^{(i)}),$$

this approximation, evaluated at each time point $t = 1, \dots, n$, is defined as the sequential approximation. Sequential importance sampling works then by approximating the target density's marginal, such that

$$p(\boldsymbol{\theta}_t | y_t) \approx \sum_{i=1}^N w_t^{(i)} \delta(\boldsymbol{\theta}_t - \boldsymbol{\theta}_t^{(i)})$$

where δ is the Dirac δ function.

Using the Markovian properties of DGLMs as mentioned in Section 1.1 we can then write a recursion for the full posterior:

$$p(\boldsymbol{\theta}_{0:t} | \mathcal{D}_t) \propto p(y_t | \boldsymbol{\theta}_t) p(\boldsymbol{\theta}_t | \boldsymbol{\theta}_{t-1}) p(\boldsymbol{\theta}_{0:t-1} | \mathcal{D}_{t-1}) \quad (2.12)$$

If we replace the decomposition (2.12) in the importance weight definition in (2.11) we have

$$w_t^{(i)} \propto \frac{p(y_t | \boldsymbol{\theta}_t^{(i)}) p(\boldsymbol{\theta}_t^{(i)} | \boldsymbol{\theta}_{t-1}^{(i)}) p(\boldsymbol{\theta}_{0:t-1}^{(i)} | \mathcal{D}_{t-1})}{\pi(\boldsymbol{\theta}_{0:t}^{(i)} | \mathcal{D}_t)}$$

In an analogous way, if we decompose the importance distribution in a recursive, such that

$$\pi(\boldsymbol{\theta}_{0:t} | \mathcal{D}_t) = \pi(\boldsymbol{\theta}_t | \boldsymbol{\theta}_{0:t-1}, \mathcal{D}_t) \pi(\boldsymbol{\theta}_{0:t-1} | \mathcal{D}_{t-1})$$

and replace in the weights expression, we get

$$w_t^{(i)} \propto \frac{p(y_t | \boldsymbol{\theta}_t^{(i)}) p(\boldsymbol{\theta}_t^{(i)} | \boldsymbol{\theta}_{t-1}^{(i)}) p(\boldsymbol{\theta}_{0:t-1}^{(i)} | \mathcal{D}_{t-1})}{\pi(\boldsymbol{\theta}_t^{(i)} | \boldsymbol{\theta}_{0:t-1}^{(i)}, \mathcal{D}_t) \pi(\boldsymbol{\theta}_{0:t-1}^{(i)} | \mathcal{D}_{t-1})}$$

If we consider the time step at $t - 1$, samples can be drawn from

$$\boldsymbol{\theta}_{0:t-1}^{(i)} \sim \pi(\boldsymbol{\theta}_{0:t-1} | \mathcal{D}_{t-1})$$

and the weights $w_{t-1}^{(i)}$ calculated. Samples $\boldsymbol{\theta}_{0:t}^{(i)}$ from the importance distribution $\pi(\boldsymbol{\theta}_{0:t} | \mathcal{D}_t)$ can then be drawn at step t as

$$\boldsymbol{\theta}_t^{(i)} \sim \pi(\boldsymbol{\theta}_t | \boldsymbol{\theta}_{0:t-1}^{(i)}, \mathcal{D}_t) \quad (2.13)$$

and the importance weights from the previous step are proportional to the last term in the previous weights

$$w_{t-1}^{(i)} \propto \frac{p(\boldsymbol{\theta}_{0:t-1}^{(i)} | \mathcal{D}_{t-1})}{\pi(\boldsymbol{\theta}_{0:t-1}^{(i)} | \mathcal{D}_{t-1})}$$

This allows the weight calculation to satisfy the recursion

$$w_t^{(i)} \propto \frac{p(y_t | \boldsymbol{\theta}_t^{(i)}) p(\boldsymbol{\theta}_t^{(i)} | \boldsymbol{\theta}_{t-1}^{(i)})}{\pi(\boldsymbol{\theta}_t^{(i)} | \boldsymbol{\theta}_{0:t-1}^{(i)}, \mathcal{D}_t)} w_{t-1}^{(i)}. \quad (2.14)$$

and the discrete approximation of $p(\cdot)$ is then

$$\hat{p}(\boldsymbol{\theta}_{0:t} | \mathcal{D}_t) \triangleq \sum_{i=1}^{N_p} w_t^{(i)} \delta(\boldsymbol{\theta}_{0:t} - \boldsymbol{\theta}_{0:t}^{(i)}), \quad (2.15)$$

$$\sum_{i=1}^{N_p} w_t^{(i)} = 1. \quad (2.16)$$

Here, $w_t^{(i)}$ is the unnormalised *importance weight*, which accounts for the differences between the target distribution (2.6) and our proposal density (2.9), given by

$$w_t^{(i)} \propto \frac{p(\boldsymbol{\theta}_t^{(i)})}{\pi(\boldsymbol{\theta}_t^{(i)})}, \quad \tilde{w}_t^{(i)} = \frac{w_t^{(i)}}{\sum_{j=1}^{N_p} w_t^{(j)}}$$

Ideally the importance density should be chosen as to minimise $\text{Var}(w_t^{(i)})$. According to [10] a common choice is the prior itself, which in the DGLM case is given by (1.4), although this is typically far from optimal.

The convergence of this method is guaranteed by the central limit theorem and the error term is $\mathcal{O}(N^{-1/2})$ regardless of the dimensionality of $\boldsymbol{\theta}$ [19].

The simplest application of IS for sequential state estimation is Sequential Importance Sampling (SIS). If the proposal can be written in the form of (2.12) importance sampling can be calculated in a sequential manner. Algorithm 1

Algorithm 1 Sequential Importance Sampling

initialisation ($t = 0$):

for $i \leftarrow 1$ to N_p

Draw $\theta_0^{(i)} \sim \mathcal{N}(\mathbf{m}_0, \mathbf{C}_0)$

Set $w_0^{(i)} = \frac{1}{N_p}$

for $t \leftarrow 1$ to k

for $i \leftarrow 1$ to N_p

Draw $\theta_t^{(i)} \sim \pi(\theta_t | \theta_{0:t-1}, \mathcal{D}_t)$

Calculate the importance weight using (2.14).

Normalise weights $w_t^{(i)} = \frac{\bar{w}_t^{(i)}}{\sum_{i=1}^{N_p} \bar{w}_t^{(i)}}$

presents a generic method to calculate $p(\theta_{0:t} | \mathcal{D}_t)$ using N_p particles.

The SIS filter will not be included in the subsequent analysis, however it represents an important framework from which other filters can be built.

2.3 Resampling

One of the drawbacks of SIS [21] is the potential inaccuracy of the estimation due to the large variance of the importance weights. Additionally, eventually all except a few particles will have a negligible weight. This is problematic both from the point of view of accuracy (since we are constructing the approximation from a few samples) and performance (computations for particles not contributing are still being executed). This is the well-known [13] problem of *weight degeneracy*, where after a few steps the majority of the weights will eventually be close to zero (as represented in Figure 2.1). The distribution (2.15) will then be eventually approximated by a very small number of particles, becoming inaccurate and with a large posterior variance. By employing resampling, *i.e.* choosing particles us-

ing their weights as a criterion, the degeneracy problem can be somewhat mitigated.

The resampling stage, while usually being independent from the state vector's dimension, is a crucial step regarding the performance of SMC implementations, impacting both the posterior variance and the computational speed. It is only natural, then, that research into resampling methods is an active area with a large variety of available implementations.

In this paper we choose three of the most common methods (multinomial [13], stratified [9] and systematic [15]) to be quantitatively analysed in Section 4.1. These selected methods belong to the category of *single-distribution, unbiased resamplers*. This *unbiasedness* means that, for a certain particle i , we expect it to be sampled $N_t^{(i)}$ times proportional to its weight $w_t^{(i)}$. That is

$$\mathbb{E} \left[N_t^{(i)} | w_t^{(i)} \right] = N w_t^{(i)}$$

We also assume that the weights available at each timepoint, prior to resampling, are normalised, this is $\sum_{i=1}^{N_p} w_t^{(i)} = 1$.

2.3.1 Resampling methods

Multinomial resampling Multinomial resampling is possibly the most common method employed in the literature. This method samples particles indices from a multinomial distribution such that

$$i^k \sim \mathcal{MN}(N_p; w^1, \dots, w^{N_p}).$$

Multinomial resampling is not, however, the most efficient resampling algorithm (as shown in [4]) with a computational complexity of $\mathcal{O}(N_p M)$.

Stratified resampling Stratified resampling [15, 9] works by generating N_p ordered random numbers

$$u_k = \frac{(k-1) + \tilde{u}_k}{N_p}, \quad \tilde{u}_k \sim \mathcal{U}[0, 1)$$

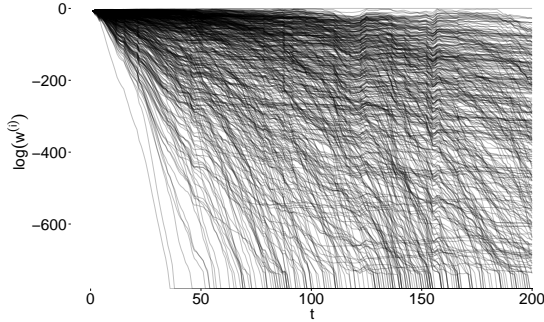


Figure 2.1: SIS particle log-weights in a local level Normal DLM for 250 iterations using simulated data. Initial weights are $1/N_p$, $N_p = 500$.

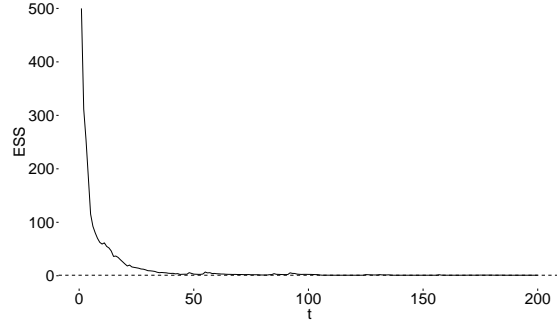


Figure 2.2: SIS (with $N_p = 500$) \widehat{ESS}_t in a local level Normal DLM for 250 iterations.

and drawing the particle indices as

$$i_k = \left\{ u_k : \sum_{n=1}^{i-1} w_n \leq u_k \leq \sum_{n=1}^i w_n \right\}. \quad (2.17)$$

Stratified resampling runs in $\mathcal{O}(N_p)$ time.

Systematic resampling Systematic resampling [15] consists of sampling a single $u_1 \sim \mathcal{U}\left[0, \frac{1}{N_p}\right]$ and setting $u_k = u_1 + \frac{k-1}{N_p}$ for $k = 1, \dots, N_p$. We then draw the particles indices, as in stratified resampling, according to (2.17).

Systematic resampling runs in $\mathcal{O}(N_p)$ time.

It is important to note that although resampling schemes alternative to multinomial do provide a smaller computational burden, they do not guarantee in practice that we will always have a smaller posterior variance [8].

2.3.2 Effective Sample Size

A standard way of quantifying weight degeneracy is to estimate the *Effective Sample Size* (ESS). The ESS can be written [20, 16, 18] as

$$ESS = \frac{N_p}{1 + N_p^2 \text{Var}\left(w_t^{(i)}\right)}.$$

From the ESS definition it is clear that this will take values between the extremes $ESS = N_p$,

which can be interpreted as all N_p particles contributing equally to the density estimation, and $ESS = 1$, interpreted as a single particle contributing to the density estimation. The usual estimate of the ESS is given by

$$\widehat{ESS}_t = \frac{1}{\sum_{i=1}^{N_p} \left(w_t^{(i)}\right)^2}. \quad (2.18)$$

This estimate also conforms to the bounds of the ESS, that is $1 \leq \widehat{ESS}_t \leq N_p$. Using this definition of ESS, we can then express it as a ratio of the total number of particles (*e.g.* half the particles contributing to the estimation would be equivalent to $\widehat{ESS}_t = N_p/2$)

Applying the ESS calculation to our SIS previous result, we get the result shown in Figure 2.2.

From this plot, we can see that the ESS starts from a value of N_p , as we have all particles initially with uniform weight of $1/N_p$, decaying to the value of $\widehat{ESS}_t \approx 1$, interpreted as a single particle contributing to the estimation.

2.3.3 Weight degeneracy vs. particle impoverishment

It is important to note that resampling does not completely solve the degeneracy problem, and in fact introduces a new problem, *particle impoverishment*. By discarding particles with lower weights we are also reducing the overall parti-

cle diversity and the number of unique particles trajectories which explore the state space. Resampling at every time-point t might be inefficient [20] and could be done only when the ESS is below a certain pre-defined threshold proportional to the number of particles (this was not the approach in our estimations in Section 4 where, for consistency, all the methods apply resampling at each time t).

Resampling also has an impact from the computational implementation point of view since, where previously in SIS all particles operations could be computed in parallel, we now have a single point of synchronisation before proceeding to the next iteration step. There are several [22, 12] resampling algorithms which allow for parallel resampling but this was considered to be outside the scope of this paper.

2.4 Sequential Importance Resampling

The *Sequential Importance Resampling* (SIR) method, introduced by Gordon *et al.* in [13] and Kitagawa *et al.* [15], tries to solve the degeneracy problem by introducing particle resampling.

The SIR algorithm also aims at calculating a discrete approximation of the state posterior, provided the model parameters are known.

While resampling might help solve the problem of particle degeneracy, it introduces a different problem, discussed in Section 2.3.3, particle impoverishment.

2.5 Auxiliary Particle Filter

The Auxiliary Particle Filter (APF), first introduced by Pitt *et al.* in [23] is an extension of SIR which aims at partially solving the problem of particle degeneracy by pre-selecting particles before propagation.

If we consider an auxiliary variable i and define [23] the target joint density to approximate as

$$p(\theta_t, i | \mathcal{D}_t) \propto p(y_t | \theta_t) p(\theta_t | \theta_{t-1}^{(i)}) w_{t-1}^{(i)},$$

Algorithm 2 Sequential Importance Resampling

initialisation ($t = 0$):

Same initialisation as SIS (Algorithm 1)

for $t \leftarrow 1$ to k

for $i \leftarrow 1$ to N_p

Draw $\theta_t^{(i)} \sim \pi(\theta_t | \theta_{0:t-1}, \mathcal{D}_t)$

Calculate the *importance weight* using (2.14).

Normalise weights $w_t^{(i)} = \frac{\tilde{w}_t^{(i)}}{\sum_{i=1}^{N_p} \tilde{w}_t^{(i)}}$

Resample according to $p(j(i) = l) = w_k$ (as discussed in Section 2.3).

for $i \leftarrow 1$ to N_p

Set $w_k^{(i)} = \frac{1}{N_p}$

then, by defining $\mu_t^{(i)}$ as some characterisation of $\theta_t | \theta_{t-1}^{(i)}$, which can be the mean, mode, a sample or some other [23] characterisation of $\theta_t | \theta_{t-1}^{(i)}$, this joint density can be approximated by

$$\pi(\theta_t, i | \mathcal{D}_t) \propto p(y_t | \mu_t^{(i)}) p(\theta_t | \theta_{t-1}^{(i)}) w_{t-1}^{(i)}, \quad (2.19)$$

with the weights proportional to

$$w_t^{(j)} \propto \frac{p(y_t | \theta_t^{(i)})}{p(y_t | \mu_t^{(i)})}.$$

The APF allows us to approximate an adapted proposal, that is taking into account y_t , when sampling is not possible from the fully adapted $\pi(\theta_t | \theta_{0:t-1}, \mathcal{D}_t)$. The SIR and the APF represent two distinct classes or algorithms, commonly referred in the literature respectively as the *sample-resample* and the *resample-sample* families, based on the order upon which the particle selection is computed. Algorithm 5, in the appendix, presents a generic method to imple-

ment the APF.

3 State and Parameter Estimation

The methods introduced in Section 2 allow us to sequentially estimate the state. However, in real world applications the model's parameters would also be unknown. Extensions to the previous algorithms would then be needed to simultaneously perform state and parameter estimation, defined by (2.1). We will introduce additional methods which will enable us to do this mainly using two different approaches, by either jointly estimating the states and parameters by incorporating the parameters in the state space (Liu and West) or by marginalising the parameters using a sufficient statistics methodology (Storvik and Particle Learning). In the following sections we will assume that although unknown, the parameters to be estimated are static, otherwise they could be incorporated into the state vector.

3.1 Liu and West's Filter

The Liu and West particle filter, first described in [17], falls into the category of joint estimation, *i.e.* by augmenting the state-space with the parameters.

One problem of trying to estimate static parameters is that, by definition, they will not change their value since $t = 1$. When estimating the parameters as a part of the state space, this will cause problems, namely a degeneracy of the particles.

An initial naive approach could be to add artificial noise to the parameters. However, this will also lead to an artificial increase in the variance of the estimates, *i.e.* the posteriors, and is essentially equivalent to assuming the parameters are slowly time varying.

The solution proposed by Liu and West [17] is to use a kernel smoothing approximation, with a correction factor to account for over-dispersion.

According to [17], we take the observation den-

sity (1.1), the transition (1.2) and assume that at time $t + 1$ we want to generate a sample from the posterior $p(\boldsymbol{\theta}_{t+1}|\mathcal{D}_{t+1})$, that is, from

$$p(\boldsymbol{\theta}_{t+1}|\mathcal{D}_{t+1}) \propto p(y_{t+1}|\boldsymbol{\theta}_{t+1}) p(\boldsymbol{\theta}_{t+1}|\mathcal{D}_t).$$

We can then rewrite the update step by using the discrete approximation to $p(\boldsymbol{\theta}_{t+1}|\mathcal{D}_t)$

$$p(\boldsymbol{\theta}_{t+1}|\mathcal{D}_{t+1}) \propto p(y_{t+1}|\boldsymbol{\theta}_{t+1}) \sum_{i=1}^{N_p} w_t^{(i)} p(\boldsymbol{\theta}_{t+1}|\boldsymbol{\theta}_t^{(i)})$$

The Liu and West (LW) filter comprises of a kernel shrinkage step to help against the variance increase caused by the Gaussian mixture.

Considering that at time t we have a SMC approximation to $p(\Phi_t|\mathcal{D}_t)$ given by the draws $\Phi_t^{(i)}$ with corresponding weights $w_t^{(i)}$, according to [25], the smoothed kernel density is given by

$$p(\Phi|\mathcal{D}_t) \approx \sum_{i=1}^{N_p} w_t^{(i)} \mathcal{N}(\Phi|\mathbf{m}_t^{(i)}, h^2 V_t) \quad (3.1)$$

In (3.1) we have a multivariate normal distribution in the form $\mathcal{N}(\cdot|\mathbf{m}, \mathbf{C})$ with mean \mathbf{m} and covariance \mathbf{C} . The sum results then in a mixture of multivariate normals weighted by their corresponding weights.

The reasoning, provided by [17], for the shrinkage approach is that without it, the kernel locations would be $\mathbf{m}_t^{(i)} = \Phi_t^{(i)}$. This would result in an over-dispersed kernel density relative to the posterior, since the variance of the mixture will be $(1 + h^2) V_t$, always bigger than V_t . This will lead to accumulation of dispersion, since an over-dispersed $p(\Phi|\mathcal{D}_t)$ will lead to even higher over-dispersion in $p(\Phi|\mathcal{D}_{t+1})$ approximation.

The kernel's moments are then calculated by

$$\mathbf{m}_t^{(i)} = a\Phi^{(i)} + (1 - a)\bar{\Phi} \quad (3.2)$$

where $a = \sqrt{1 - h^2}$ and $h > 0$ is the smoothing parameter and the variance by

$$V_t = \sum_{i=1}^{N_p} \frac{(\Phi^{(i)} - \bar{\Phi})(\Phi^{(i)} - \bar{\Phi})^T}{N_p} \quad (3.3)$$

with $\bar{\Phi} = \sum_{i=1}^N \Phi^{(i)} / N_p$. With this method, the mean $\bar{\Phi}_t$ is kept and having correct variance V_t , correcting the over-dispersion. A summary for the steps of the Liu and West filter is presented in Algorithm 6 in the appendix.

By propagating the parameter proposals with a MVN impulse we can apply LW to any class of state-space models.

3.2 Storvik Filter

The Storvik filter, first presented in [24] and related to [11], unlike Liu & West does not incorporate parameters in the state vector but instead works by assuming that the posterior $p(\Phi | \mathcal{D}_t, \theta_{0:t})$ depends on a set of sufficient statistics (SS) s_t with an associated recursive update. By performing parameter estimation based on this set of sufficient statistics and separately from the state estimation, the Storvik filter aims at reducing particle impoverishment while reducing computational load due to the low-dimensionality of s_t [24]. The deterministic update of s_t will depend on the state estimates and parameter estimates, such that $s_t = \mathcal{S}(s_{t-1}, \theta_t, \theta_{t-1}, y_t)$.

According to [24], we use the decomposition

$$p(\theta_{0:t}, \Phi | \mathcal{D}_t) = C \cdot p(\theta_{0:t-1} | \mathcal{D}_{t-1}) p(\Phi | s_{t-1}) \times p(\theta_t | \theta_{t-1}, \Phi) p(y_t | \theta_t, \Phi), \quad (3.4)$$

where $C = [p(y_t | \mathcal{D}_{t-1})]^{-1}$ which is a constant not depending on $\theta_{0:t}$ or Φ .

Simulation from 3.4 can be performed with the additional step that Φ also needs to be simulated. The simplest way to simulate from 3.4 is to draw from

$$\begin{aligned} \theta_{0:t-1} &\sim p(\theta_{0:t-1} | \mathcal{D}_{t-1}) \\ \Phi &\sim p(\Phi | s_{t-1}) \\ \theta_t &\sim p(\theta_t | \theta_{0:t-1}, \Phi) \end{aligned}$$

and accept with probability $p(y_t | \theta_t, \Phi)$. The steps of the Storvik filter are summarised in Algorithm 7 in the appendix.

Although Storvik works in a *sample-resample* framework, it can also be applied within a *resample-sample* framework.

3.3 Particle Learning

Particle Learning (PL), first introduced in [5] employs a similar sufficient statistics mechanism as Storvik, although within a resample-sample framework. Unlike Storvik, where sufficient statistics structure is used solely for estimating parameters, in PL the state can also marginalised if a sufficient statistics structure is available for the state. This means that prior to sampling from the proposal distribution, we resample the current state particles and sufficient statistics taking y_{t+1} into account, using a predictive likelihood. A general implementation for a Particle Learning is presented in Algorithm 8 in the appendix.

Particle Learning promises to reduce the problem of particle impoverishment, although in practice it does not solve the problem completely [6].

3.4 Sufficient Statistics

An example for sufficient statistics can be given using the Poisson DLM with a locally constant model evolution. The general model is given by Section 1.1. Considering the model evolution, where $F_t = F = [1]$ and $G_t = G = [1]$, we then have

$$\begin{aligned} y_t | \Phi, \lambda_t &\sim \text{Po}(\lambda_t) \\ \lambda_t | \theta_t &= \exp\{\theta_t\} \\ \theta_t | \Phi, \theta_{t-1} &\sim \mathcal{N}(\theta_{t-1}, \sigma^2) \end{aligned}$$

Using an inverse Gamma prior for $\sigma_0^2 \sim \mathcal{IG}(\alpha_0, \beta_0)$ we have a semi-conjugate update leading to $\sigma^2 | \theta_{0:n} \sim \mathcal{IG}(\alpha_0 + \frac{n}{2}, \beta_0 + \frac{1}{2} \sum_{i=1}^n (\theta_i - \theta_{t-1})^2)$. From this we can extract the necessary quantities as

$$s_t = \begin{bmatrix} n \\ (\theta_t - \theta_{t-1})^2 \end{bmatrix}$$

Algorithm 3 State forecasting

for $\tau \leftarrow 1$ to k

 for $i \leftarrow 1$ to N_p

Sample

$$\tilde{\theta}_{t+\tau}^{(i)} \sim p\left(\theta_{t+\tau} | \theta_{0:t+(\tau-1)}^{(i)}, \mathcal{D}_t, \Phi_t^{(i)}\right)$$

And perform the draws for $\Phi^{(i)}$ as

$$\Phi^{(i)} \sim \mathcal{IG}\left(\alpha + \frac{1}{2}s_{0,t}^{(i)}, \beta + \frac{1}{2}s_{1,t}^{(i)}\right)$$

It is important to note that the sufficient statistics method does not solve entirely the degeneracy and impoverishment problems, since we are still applying resampling methods to the set s_t .

3.5 Forecasting

We will denote k -step ahead forecasting, considering we have observations until the current time t , predicting states or observations up to time $t + \tau$, where $\tau = 1, \dots, k$.

State forecasting State forecasting with SMC methods can be performed by carrying the model forward without performing resampling or reweighting (since we are not in possession of observations $y_{t+1:t+k}$).

If we consider the current marginal posteriors for both the states and parameters, that is $p(\theta_t | y_t, \Phi_t^{(i)})$ our aim is then to estimate $p(\theta_{t+1:t+k} | y_t, \Phi_t^{(i)})$, and since we are considering our parameters as static, this is done according to Algorithm 3.

It is worth noting that within the proposed DGLM framework, the Algorithm 3 will work directly, since our importance density $\tilde{\theta}_{t+\tau}^{(i)} \sim p(\theta_{t+\tau} | \theta_{0:t+(\tau-1)}^{(i)}, \mathcal{D}_t, \Phi_t^{(i)})$ is in the form of (1.4). However, fully adapted proposals will not

be directly applicable, since they will be conditioned on $\mathcal{D}_{t+1:t+\tau}$, which is not yet available at t .

3.6 Particle Marginal Metropolis-Hastings

As mentioned previously, these SMC methods will be benchmarked against a “gold standard” off-line method, namely Particle Marginal Metropolis-Hastings (PMMH) [1].

If we consider the joint distribution $p(\theta_{0:T}, \Phi | \mathcal{D}_t)$, ideally (if sampling from $p(\theta_{0:T} | \mathcal{D}_t, \Phi)$ were possible), we would simply sample from the joint proposal

$$\pi((\theta'_{0:T}, \Phi') | (\theta_{0:T}, \Phi)) = \pi(\Phi' | \Phi) p(\theta'_{0:T} | \mathcal{D}_t, \Phi'),$$

requiring only the specification of a proposal $\pi(\Phi' | \Phi)$ for the construction of the sampler. Since we cannot, generally, sample directly from $p(\theta_{0:T} | y_{1:T}, \Phi)$ or calculate $p(\mathcal{D}_t | \Phi)$ directly, PMMH works by using SMC approximations to these quantities. With the approximation $\hat{p}(\mathcal{D}_t | \Phi)$ and a sampled trajectory $\Theta_{0:T}$ we can then calculate the Metropolis-Hastings acceptance ratio

$$\min \left\{ \frac{\hat{p}(\mathcal{D}_T | \Phi') \pi(\Phi') \pi(\Phi | \Phi')}{\hat{p}(\mathcal{D}_T | \Phi) \pi(\Phi) \pi(\Phi' | \Phi)} \right\} \quad (3.5)$$

Pseudo-marginal arguments show that despite the use of approximate estimates, the sampler nevertheless has the exact posterior as its target.

PMMH is presented in algorithm 4, where ℓ_0 and ℓ_{acc} indicate, respectively, the initial and accepted estimates of $\hat{p}(\mathcal{D}_t | \Phi)$.

4 Results

The datasets used for the tests of the algorithms’ implementation aim at covering the three main observation models discussed, Normal, Poisson and Binomial.

For the Normal case we have chosen a continuous measurement dataset, namely a series of

Algorithm 4 PMMH algorithm

initialisation;

With initial parameters Φ_0 and $\mathbf{m}_0, \mathbf{C}_0$ run
a SIR filter and store $\left\{\boldsymbol{\theta}_{0:T}^{(k)}\right\}_0, \ell_0$;

Set $\ell_{acc} \leftarrow \ell_0$ and $\Phi_{acc} \leftarrow \Phi_0$;

for $n \leftarrow 1$ to N_{iter}

Propose new parameters

$$\Phi_n \sim \mathcal{N}(\Phi_{acc}, \mathbf{C}_{step})$$

Run a SIR with parameters Φ_n and store
 $\left\{\boldsymbol{\theta}_{0:T}^{(k)}\right\}_n, \ell_n$

Draw $r \sim \mathcal{U}(0, 1)$

if $\log(r) < (\ell_n - \ell_{acc})$

$\ell_{acc} \leftarrow \ell_n$

$\Phi_{acc} \leftarrow \Phi_n$

temperature measurements with 5 minute intervals from the city Austin, Texas (USA) captured by the National Oceanic and Atmospheric Administration¹ (NOAA) [7] shown in Figure 4.2.

For the Poisson case we have used web server log data, converted from event time to time series as to represent web hits per second. The source² of the log data is HTTP requests to the 1998 World Cup server from April 30, 1998 and July 26, 1998 [2]. A subset corresponding to May 1998 was used.

The data used for binomial data modelling comes from the US Department of Transportation's Bureau of Transport Statistics³ and consist on airport departure times. Since the data consists of scheduled and actual departure times

¹http://www1.ncdc.noaa.gov/pub/data/uscrn/products/subhourly01/2015/CRNS0101-05-2015-TX_Austin_33_NW.txt [Accessed 23/8/2016]

²<http://ita.ee.lbl.gov/html/contrib/WorldCup.html> [Accessed 23/8/2016]

³http://www.transtats.bts.gov/DL_SelectFields.asp?Table_ID=236&DB_Short_Name=On-Time

we dichotomised the dataset into binary data corresponding to *delayed* and *on-time* flights. A flight was considered delayed if it departed 30 minutes or more after the scheduled time. The data was then converted into a time series with intervals of one minute and missing observations are recorded if no departure happened. The airport chosen was the JFK airport in New York City and the period was January 2015.

The Mean Squared Error (MSE) for each single state vector component for each model was compared. The state's MSE was calculated using the PMMH estimation values as

$$\text{MSE}_i = \frac{1}{N_{obs}} \sum_{t=1}^{N_{obs}} \left(\bar{\theta}_{i,t}^{PF} - \bar{\theta}_{i,t}^{PMMH} \right)^2.$$

The resampling algorithm used throughout this section was systematic resampling, as defined in Section 2.3.1, applied at each time t .

4.1 Resampler benchmarks

The ESS and posterior variance for different resampling algorithms (detailed in Section 2.3.1) was calculated using a subset ($N_{obs} = 1000$) of the temperature data and a Storvik filter with $N_p = 2 \times 10^4$ particles and model as specified in Section 4.2. There was no substantial difference in terms of ESS when using Systematic, Stratified or Multinomial resamplers (Figure 4.1). The average ESS values were respectively 1185.349, 1159.503 and 1121.302.

Regarding execution times, systematic and stratified resampling also had an advantage over multinomial resampling respectively 519.5 and 518.1 seconds, against 639.3 seconds. Following these results we have chosen to use systematic resampling throughout the subsequent sections.

4.2 Temperature data

The temperature dataset includes erroneous measurements of either 100°C or 0°C, clearly visible in figure 4.2.

Below is the estimation for the states and parameters for the temperature data described in

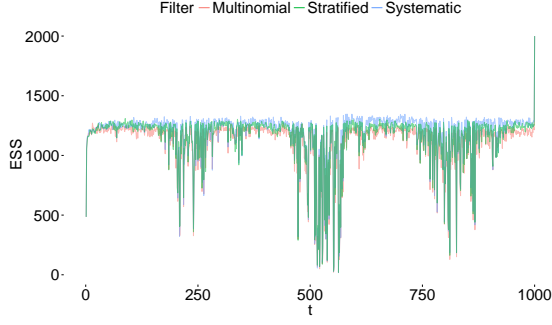


Figure 4.1: ESS for different resampling methods using Storvik ($N_p = 2000$) with a Normal DLM on a subset of the temperature data

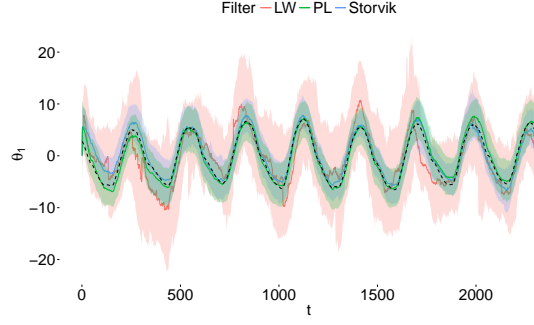


Figure 4.3: $\theta_{1:T}^2$ state component estimation for the temperature data for Storvik, PL and LW filters ($N_p = 5000$). Shaded area represents 95% coverage. Dashed line represents the PMMH estimation.

Section 4.

The estimation was performed using three of the filters (LW, Storvik and PL) with $N_p = 5000$ and $N_p = 100$. The dataset consisted of $N_{obs} = 2034 \approx 7$ days, in a dataset region without the presence of extreme values corresponding to the period between 7th and 18th July 2015.

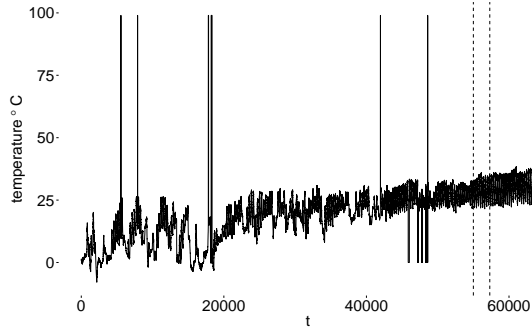


Figure 4.2: NOAA temperature data for Austin, Texas (January-July 2015) with 5 minute sampling interval.

The model used was a Normal DLM, as specified in Section 1.1, with a structure consisting of a locally constant (LC) component with a daily Fourier seasonal component ($p = 288$) with a single harmonic. The corresponding model struc-

ture is

$$\mathbf{F} = \begin{bmatrix} 1 \\ 1 \\ 0 \end{bmatrix}^T \quad \mathbf{G} = \begin{bmatrix} 1 & 0 & 0 \\ 0 & \cos(2\pi/p) & \sin(2\pi/p) \\ 0 & -\sin(2\pi/p) & \cos(2\pi/p) \end{bmatrix},$$

with a parameter set $\Phi = \{W, V\}$, where

$$V = \sigma^2 \quad W = \begin{bmatrix} \tau_{LC}^2 & 0 & 0 \\ 0 & \tau_{S1,1}^2 & 0 \\ 0 & 0 & \tau_{S1,2}^2 \end{bmatrix}.$$

The observation and state models are

$$\begin{aligned} p(y_t | \eta_t, \Phi) &= \mathcal{N}(\eta_t, \sigma^2) \\ \eta_t &= \mathbf{F}^T \boldsymbol{\theta}_t \\ p(\boldsymbol{\theta}_t | \boldsymbol{\theta}_{t-1}, \Phi) &= \mathcal{N}(\mathbf{G}\boldsymbol{\theta}_{t-1}, W) \end{aligned}$$

The state priors were $\boldsymbol{\theta}_0 \sim \mathcal{N}((20, 0, 0)^T, 10\mathbf{I}_3)$ in order to cover an acceptable range of temperatures for the chosen period, and the parameter priors where $\sigma_0^2 \sim \mathcal{IG}(1, 1)$ and $W_0 \sim \mathcal{IW}(3, \mathbf{I}_3)$. For LW we have used $\delta = 0.98$ as a smoothing parameter, the recommended general value [17].

Regarding state estimation we see in Table 1 that both sufficient statistics based methods have a consistently lower MSE across the state

N_p	MSE	$Filter$		
		LW	Storvik	PL
5000	θ^1	6.66	1.511	0.6512
	θ^2	6.556	1.507	0.6538
	θ^3	6.442	1.378	1.298
	iteration (ms)	8.138	22.75	25.5
100	θ^1	199.6	7.014	4.246
	θ^2	199.0	7.064	4.193
	θ^3	546.5	7.878	4.192
	iteration (ms)	0.4683	0.566	0.6137

Table 1: State estimation MSE compared to PMMH and computation times for the temperature data using a Normal DLM

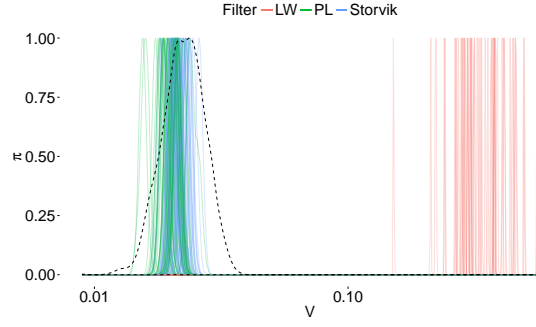


Figure 4.4: σ^2 posterior at $t = N_{obs}$ (log-scale) for 50 runs with the temperature data with $N_p = 5000$ (LW, Storvik, PL compared to PMMH)

components when compared to LW. The estimation for the state component $\theta_{1:T}^2$ is on Figure 4.3.

In terms of the ESS, PL dominates the other methods, with the mean values for LW, Storvik and PL being respectively 1202.8, 2839.3 and 4575.9. In terms of computational times, Storvik and PL have costs in the same order of magnitude, while LW is the least costly of the three methods.

Additionally, the estimation was performed with a very low number of particles ($N_p = 100$) where the difference between the SS based method accentuates in comparison with LW (Table 1). The former still produce an acceptable state estimation whereas the latter, due to the filter's collapse fails to provide a reasonable estimation.

In figure 4.4 we show the σ^2 posterior at $t = N_{obs}$ for 50 runs of each filter where it is visible that SS based methods fall within the PMMH estimated values but that they grossly underestimate the true posterior variance. The early collapse of LW is clearly visible in Figure 4.5.

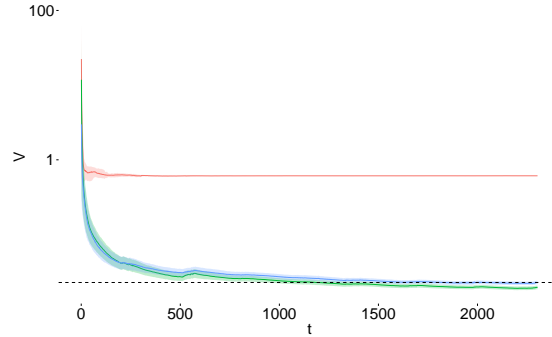


Figure 4.5: σ^2 means and 95% coverage for the temperature data using a Normal DLM ($N_p = 5000$). Dashed line represents PMCMC estimation.

The MSE between the one-step ahead observation forecast and the actual observation, calculated using $MSE = 1/N_{obs} \sum_{t=1}^{N_{obs}} (y_t - \hat{y}_t)^2$, was, respectively for LW, Storvik and PL, 0.0582, 0.05795, 0.0578. We can see in Figure B.1 in the appendix the one-step ahead forecast errors.

The state (Figure C.1 in the appendix) and observation (Figure 4.6) forecast, when compared respectively to the actual filtered values and observations, fall within the expected range. The forecast is performed in this case for $k = 2500$ steps, roughly equivalent to 8 days.

Regarding the state estimation's MSE variation with the number of particles, we can see (Figure 4.7) a sharp decline for low values of N_p ,

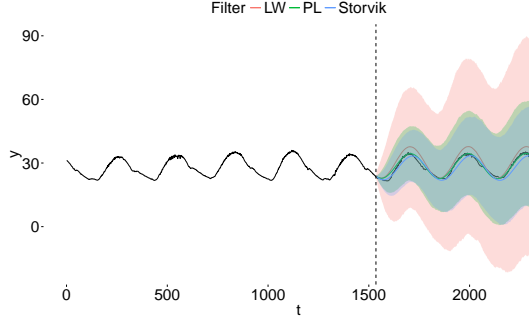


Figure 4.6: Observation forecast for the temperature dataset (Normal DLM). Shaded areas represent 95% coverage for each filter

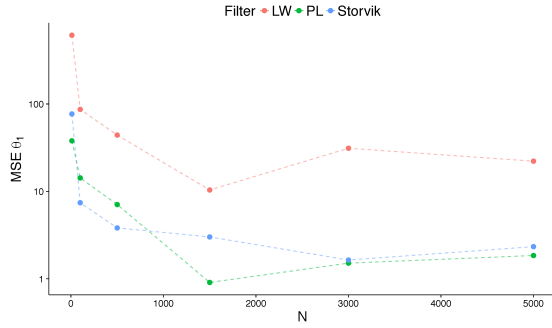


Figure 4.7: $\theta_{1:T}^1$ MSE relative to PMMH for LW, PL and Storvik with increasing N_p .

after which there seems to be no improvement. This is in conformity to the expected theoretical Monte Carlo errors which are proportional to $\frac{C_T}{\sqrt{N}}$ where C_T is a constant dependent on the choice of priors and parameters [3]. This result was consistent across the remaining estimations with different datasets and models.

4.3 Airport flight delay data

The airport delay data (Figure 4.8) was modelled using a Binomial DLM. The three filters used were LW, Storvik and PL each with $N_p = 5000$ and $N_p = 500$. The dataset's size was $N_{obs} = 4320 \approx 3$ days. The time-series' structure consists of a LC component plus a daily seasonality

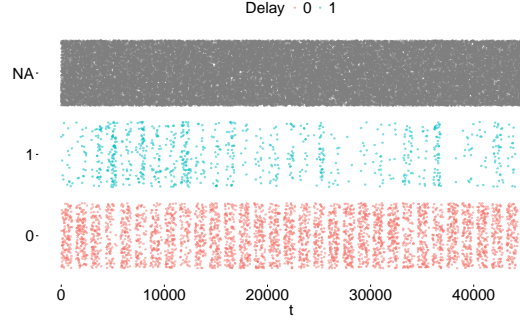


Figure 4.8: Airport delay data (January 2015, JFK airport)

($p = 1440$) with a single harmonic. The observation and state model correspond to

$$F = \begin{bmatrix} 1 \\ 1 \\ 0 \end{bmatrix}^T \quad G = \begin{bmatrix} 1 & 0 & 0 \\ 0 & \cos(2\pi/p) & \sin(2\pi/p) \\ 0 & -\sin(2\pi/p) & \cos(2\pi/p) \end{bmatrix}. \quad (4.1)$$

In this model the parameter set to estimate is $\Phi = \{W\}$ where

$$W = \begin{bmatrix} \tau_{LC}^2 & 0 & 0 \\ 0 & \tau_{S1,1}^2 & 0 \\ 0 & 0 & \tau_{S1,2}^2 \end{bmatrix}.$$

The observation and state models are

$$\begin{aligned} p(y_t | \eta_t, \Phi) &= B(1, \eta_t) \\ \eta_t &= \text{logit}^{-1}(F^T \theta_t) \\ p(\theta_t | \theta_{t-1}, \Phi) &= \mathcal{N}(G\theta_{t-1}, W) \end{aligned}$$

The same priors as with the temperature data in 4.2 were used for the parameters with a state prior $\theta_0 \sim \mathcal{N}(\mathbf{0}, 4\mathbf{I}_3)$.

Due to the high number of missing observations ($\approx 88\%$), the state estimation (Figure 4.9) displays a high MSE when compared to a PMMH run as well as poor parameter estimation (Figures 4.10 and 4.11). This is to be expected since for every missing observation we are simply propagating the states forward, using (1.4) and by-

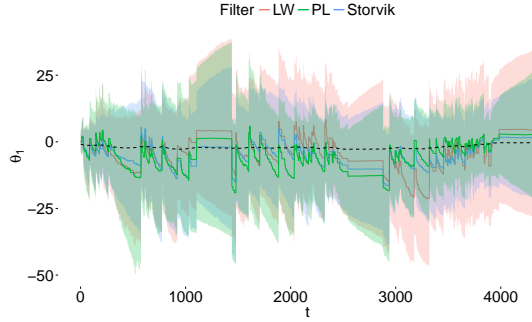


Figure 4.9: $\theta_{1:T}^1$ state component estimation for the airport delay data for Storvik, PL and LW filters. Shaded area represents 95% coverage. Noted that the (dashed) PMMH estimate is the smoothing estimate, and therefore not directly comparable with the filtered estimates.

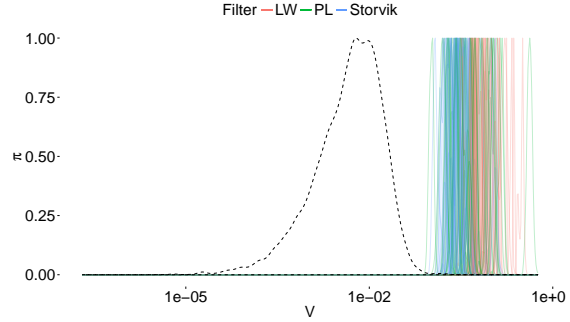


Figure 4.10: W^1 posterior at $t = N_{obs}$ (log-scale) for 50 runs with the airport data with $N_p = 5000$ (LW, Storvik, PL) compared to PMMH (dashed line)

N_p	MSE	<i>Filter</i>		
		LW	Storvik	PL
5000	θ^1	39.05	31.15	14.74
	θ^2	46.68	35.44	10.32
	θ^3	33.16	27.01	13.14
	iteration (<i>ms</i>)	4.626	5.396	5.701
500	θ^1	100.6	34.79	64.93
	θ^2	71.24	44.58	33.34
	θ^3	103.0	49.23	50.6
	iteration (<i>ms</i>)	0.2068	0.1463	0.1482

Table 2: $\theta_{1:t}^1$ MSE compared to PMMH for the airport data using a Binomial DLM

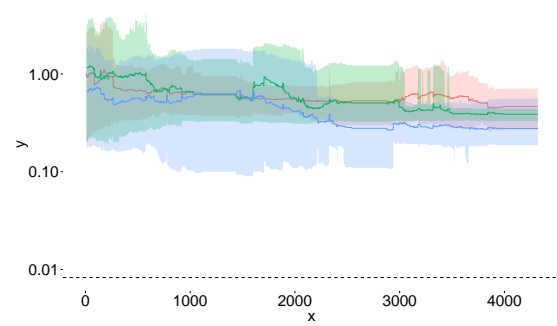


Figure 4.11: W^1 means and 95% coverage (shaded area) for the airport dataset using a Binomial DLM ($N_p = 5000$). Dashed line represents PMCMC estimation.

passing resampling. In these conditions, however, we can still see (Table 2) that sufficient statistics based methods perform generally better than LW, whereas LW, in terms of computational time is less costly.

Regarding the ESS for LW, Storvik and PL the average value was respectively 4300.34, 3892.46 and 4708.0 for $N_p = 5000$ and 414.7, 389.27 and 471.70 for $N_p = 500$.

A long term state forecast was produced according to algorithm 3 for 3360 data points, corresponding to approximately 56 hours. The resulting forecast was then compared against the actual state estimation for that period (Figure 4.12). The PL state forecast was closer to the PMMH estimation and had a smaller variance than the remaining methods.

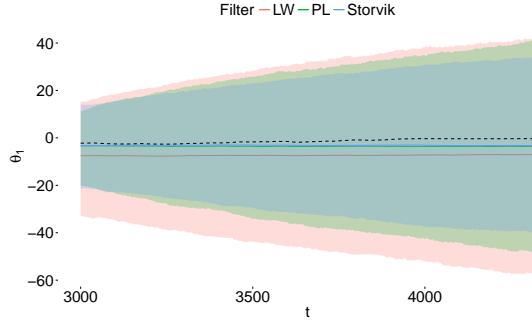


Figure 4.12: θ^1 state forecast for the airport delay compared to state estimation. Shaded area represents 95% coverage.

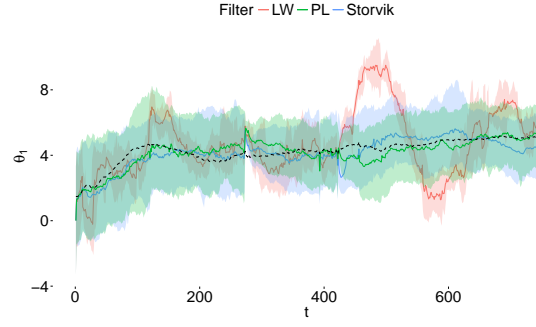


Figure 4.14: $\theta_{1:T}^1$ state estimation ($N_p = 5000$) for the WC98 data using a Poisson DLM. Shaded area represents 95% coverage. Dashed line represents the PMMH estimation.

4.4 World Cup 98 Web server data

The WC98 dataset (figure 4.13) consists of $N_{obs} = 743 \approx 31$ days of hourly measurements and exhibits both a daily and weekly pattern.

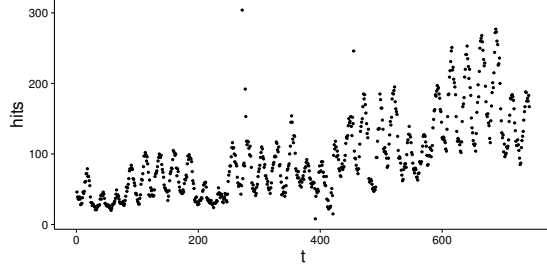


Figure 4.13: WC98 server hits (May 1998)

The estimation was performed using three of the filters (LW, Storvik and PL) with $N_p = 5000$. The model used was Poisson DLM, with a structure consisting of a locally constant (LC) component with a daily Fourier seasonal ($p_d = 24$) and weekly ($p_w = 168$) components, both with a single harmonic. Considering, $J_2(1, \omega) = \begin{bmatrix} \cos(\omega) & \sin(\omega) \\ -\sin(\omega) & \cos(\omega) \end{bmatrix}$ and $\omega = 2\pi/p$, the corre-

sponding model structure is

$$F = \begin{bmatrix} 1 & 1 & 0 & 1 & 0 \end{bmatrix},$$

$$G = \begin{bmatrix} 1 & 0 & 0 \\ 0 & J_2(1, \omega_d) & 0 \\ 0 & 0 & J_2(1, \omega_w) \end{bmatrix}$$

with a parameter set $\Phi = \{W\}$, where

$$\text{diag}(W) = \begin{bmatrix} \tau_{LC}^2 & \tau_{d1,1}^2 & \tau_{d2,2}^2 & \tau_{w1,1}^2 & \tau_{w2,2}^2 \end{bmatrix}. \quad (4.2)$$

The observation and state models are

$$p(y_t | \eta_t, \Phi) = \text{Po}(\eta_t)$$

$$\eta_t = \exp \{F^T \theta_t\}$$

$$p(\theta_t | \theta_{t-1}, \Phi) = \mathcal{N}(G\theta_{t-1}, W)$$

The state priors were $\theta_0 \sim \mathcal{N}(0, 5I_5)$ and the parameter priors where and $W_0 \sim \mathcal{IW}(5, I_5)$. As previously, for the LW we have used $\delta = 0.98$ as a smoothing parameter.

For state estimation (Figure 4.14) we can see that the SS based methods dominate in terms of MSE when compared to the PMMH estimation and LW has a slight advantage in term of computational cost (Table 3).

Regarding parameter estimation, SS methods also provide a better approximation to the

N_p	MSE	$Filter$		
		LW	Storvik	PL
5000	θ^1	3.283	0.2721	0.2609
	θ^2	0.4034	0.03121	0.02645
	θ^3	0.3286	0.04591	0.03601
	θ^4	3.168	0.2462	0.2342
	θ^5	5.532	0.2432	0.2329
	iteration (ms)	4.626	5.396	5.701

Table 3: $\theta_{1:T}$ filter estimates MSE compared to PMMH for the WC98 data using a Poisson DLM.

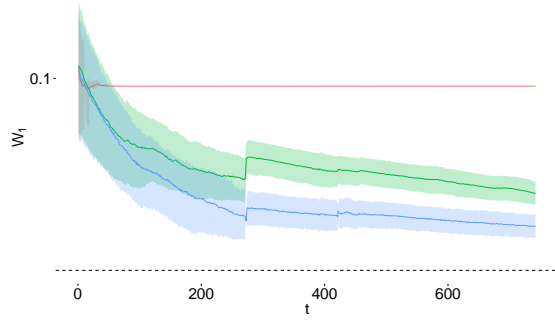


Figure 4.15: W^1 estimation history for the WC98 data using a Poisson DLM ($N_p = 5000$). Shaded area represents 95% coverage. Dashed line represents PMMH estimation.

PMMH result. There is a clear particle filter collapse for Liu and West in the early stages of the estimation (Figure 4.15) which accounts for the poor parameter estimations (Figure 4.16).

When performing a state forecast for $k = 600 \approx 6$ days, we can see (Figure 4.17) that while sufficient statistics based methods capture the seasonal patterns Liu and West does not, on account of the filter's early collapse.

5 Conclusions

Considering that we performed long run state forecasts (namely, in the temperature data we forecasted ≈ 2.65 days from data sampled every five minutes) the forecasted values were in line with the observed data.

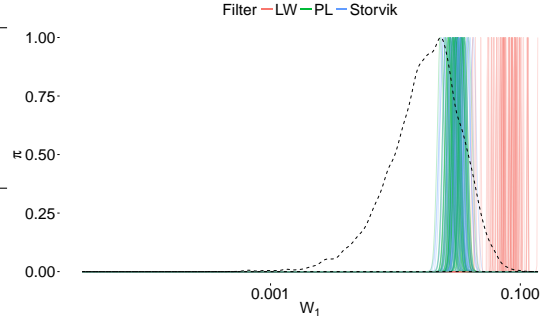


Figure 4.16: W^1 posterior at time $t = N_{obs}$ for the WC98 data using a Poisson DLM and $N_p = 5000$, using 50 runs. Dashed line represents PMMH estimation.

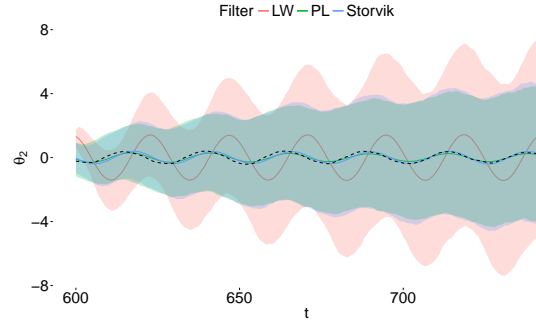


Figure 4.17: State forecast for the WC98 data

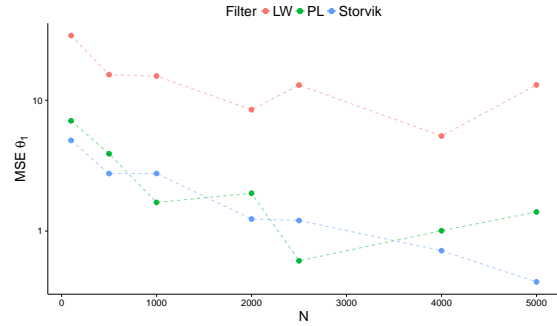


Figure 4.18: $\theta_{1:T}^1$ MSE with varying N_p for the WC98 dataset using a Poisson DLM.

The Liu and West method, suffered from a problem where the parameter estimation tended to collapse to a single value after a few hundred iterations. This is mainly due to the depletion of particles, *i.e.* particle impoverishment. Since sufficient statistics methods did not incorporate the parameters directly in the state space, particle impoverishment could be delayed for much longer.

Liu and West’s main appeal, the ability to perform state and parameter estimation in all state-space models, even when no sufficient statistics structure can be specified, does not apply to our DGLM scenario. However, Liu and West did outperform the remaining methods when the criteria was computation time.

Even though the parameter estimations fall within a certain range of the PMMH estimations, they did not offer results which could justify the substitution of standard off-line methods, such as PMMH for parameter estimation. It is however justified in the proposed scenario of inference for streaming data to use these methods, specifically those based on sufficient statistics, as it is common to try to achieve a compromise between computational times and accuracy.

These methods provided acceptable results for one-step ahead, short and even medium term forecasts. A desirable property for the application of SMC in analytics is the ability to perform trade-offs between computational costs and estimation accuracy. SS based methods show the capability of performing reasonable state estimations and forecasts, parameter estimation and consequently observation forecasts with a particle number as low as $N_p = 100$ with a computational cost in the order of milliseconds per iteration. This can prove extremely valuable when implementing such methods in low powered devices.

Acknowledgement

Rui Vieira is supported by a studentship funded by Red Hat Ltd. / JBoss.

References

- [1] C. Andrieu, A. Doucet, and R. Holenstein. Particle Markov chain Monte Carlo methods. *Journal of the Royal Statistical Society: Series B (Statistical Methodology)*, 72(3):269–342, 2010.
- [2] M. Arlitt and T. Jin. A workload characterization study of the 1998 world cup web site. In *IEEE network*, volume 14, pages 30–37. IEEE, 1996.
- [3] A. Brockwell, P. Del Moral, and A. Doucet. Sequentially interacting markov chain monte carlo methods. *The Annals of Statistics*, 38(6):3387–3411, 2010.
- [4] J. Carpenter, P. Clifford, and P. Fearnhead. Improved particle filter for nonlinear problems. *IEE Proceedings - Radar, Sonar and Navigation*, 146(1):2–7, 1999.
- [5] C.M. Carvalho, M.S. Johannes, H.F. Lopes, and N.G. Polson. Particle Learning and Smoothing. *Statistical Science*, 25(1):88–106, 2010.
- [6] N. Chopin, A. Iacobucci, J.-M. Marin, K. Mengersen, C. P. Robert, R. Ryder, and C. Schäfer. On Particle Learning. *arXiv preprint arXiv:1006.0554*, (2008):14, jun 2010.
- [7] H.J. Diamond, T.R. Karl, M.A. Palecki, C.B. Baker, J.E. Bell, R.D. Leeper, D.R. Easterling, J.H. Lawrimore, T.P. Meyers, M.R. Helfert, G. Goodge, and P.W. Thorne. U.S. climate reference network after one decade of operations status and assessment. *Bulletin of the American Meteorological Society*, 94(4):485–498, apr 2013.
- [8] R. Douc and O. Cappe. Comparison of resampling schemes for particle filtering. *ISPA 2005. Proceedings of the 4th International Symposium on Image and Signal Processing and Analysis, 2005*, pages 64–69, 2005.

- [9] A. Doucet, N. de Freitas, and N.J. Gordon. Sequential Monte Carlo Methods in Practice. *Technometrics*, page 583, 2001.
- [10] A. Doucet, S. Godsill, and C. Andrieu. On sequential Monte Carlo sampling methods for Bayesian filtering. *Statistics and Computing*, 10(3):197–208, 2000.
- [11] P. Fearnhead. Markov chain Monte Carlo, sufficient statistics, and particle filters. *Journal of Computational and Graphical Statistics*, 11(4):848–862, 2002.
- [12] P. Gong, Y. O. Basciftci, and F. Ozguner. A parallel resampling algorithm for particle filtering on shared-memory architectures. In *Proceedings of the 2012 IEEE 26th International Parallel and Distributed Processing Symposium Workshops, IPDPSW 2012*, pages 1477–1483. IEEE, IEEE, may 2012.
- [13] N.J. Gordon, D.J. Salmond, and A.F.M. Smith. Novel approach to nonlinear/non-Gaussian Bayesian state estimation. *IEE Proceedings F-Radar and Signal Processing*, 140(2):107–113, 1993.
- [14] R.E. Kalman. A new approach to linear filtering and prediction problems. *Journal of basic Engineering*, 82(1):35–45, 1960.
- [15] G. Kitagawa. Monte Carlo filter and smoother for non-Gaussian nonlinear state space models. *Journal of computational and graphical statistics*, 5(1):1–25, 1996.
- [16] A. Kong, J.S. Liu, and W.H. Wong. Sequential imputations and Bayesian missing data problems. *Journal of the American statistical association*, 89(425):278–288, 1994.
- [17] J. Liu and M. West. Combined parameter and state estimation in simulation-based filtering. In *Sequential Monte Carlo Methods in Practice*, pages 197–223. Springer, 2001.
- [18] J.S. Liu. Metropolized independent sampling with comparisons to rejection sampling and importance sampling. *Statistics and Computing*, 6(2):113–119, 1996.
- [19] J.S. Liu. *Monte Carlo strategies in scientific computing*. Springer Science & Business Media, 2002.
- [20] J.S. Liu and R. Chen. Sequential Monte Carlo methods for dynamic systems. *Journal of the American statistical association*, 93(443):1032–1044, 1998.
- [21] S.N. Maceachern, M. Clyde, and J.S. Liu. Sequential importance sampling for non-parametric Bayes models: The next generation. *Canadian Journal of Statistics*, 27(2):251–267, 1999.
- [22] L.M. Murray, A. Lee, and P.E. Jacob. Parallel resampling in the particle filter. *Journal of Computational and Graphical Statistics*, 2015:21, jan 2015.
- [23] M.K. Pitt and N. Shephard. Filtering via simulation: Auxiliary particle filters. *Journal of the American statistical association*, 94(446):590–599, 1999.
- [24] G. Storvik. Particle filters for state-space models with the presence of unknown static parameters. *IEEE Transactions on signal Processing*, 50(2):281–289, 2002.
- [25] M. West. Mixture models, Monte Carlo, Bayesian updating, and dynamic models. *Computing Science and Statistics*, pages 325–325, 1993.
- [26] M. West and J. Harrison. *Bayesian Forecasting and Dynamic Linear Models*. Springer series in statistics. Springer, New York, NY [u.a.], 1997.

A Algorithms

Algorithm 5 Auxiliary Particle Filter

```

initialisation;
for  $t \leftarrow 1$  to  $k$  do
  for  $i \leftarrow 1$  to  $N_p$  do
    Calculate  $\mu_t^{(i)}$ 
    Calculate  $\tilde{w}_t^{(i)} \propto p(y_t | \mu_t^{(i)}) w_{t-1}^{(i)}$ 
  end for
  Normalise weights:  $w_t^{(i)} = \frac{\tilde{w}_t^{(i)}}{\sum_{i=1}^{N_p} \tilde{w}_t^{(i)}}$ 
  Resample according to  $p(j(i) = l) = w_t$ 
  (as discussed in Section 2.3).
  for  $i \leftarrow 1$  to  $N_p$  do
    Draw  $\theta_t^{(i)} \sim p(\theta_t | \theta_{t-1}^{i(j)})$ 
    Calculate  $\tilde{w}_t^{(i)} = \frac{p(y_t | \theta_t^{(i)})}{p(y_t | \mu_t^{i(j)})}$ 
  end for
  Normalise weights:  $w_t^{(i)} = \frac{\tilde{w}_t^{(i)}}{\sum_{i=1}^{N_p} \tilde{w}_t^{(i)}}$ 
end for

```

Algorithm 6 Liu and West

```

initialisation;
for  $t \leftarrow 1$  to  $k$  do
  for  $i \leftarrow 1$  to  $N_p$  do
    Calculate  $\mu_t^{(i)}$ 
    Calculate  $\mathbf{m}_{t-1}$  according to 3.2
    Calculate  $V_{t-1}$  according to 3.3
    Calculate
       $\tilde{w}_t^{(i)} \propto p(y_t | \mu_t^{(i)}, \mathbf{m}_{t-1}^{(i)}) w_{t-1}^{(i)}$ 
  end for
  Normalise weights:  $w_t^{(i)} = \frac{\tilde{w}_t^{(i)}}{\sum_{i=1}^{N_p} \tilde{w}_t^{(i)}}$ 
  Resample according to  $p(j(i) = l) = w_t$ 
  (as discussed in Section 2.3).
  for  $i \leftarrow 1$  to  $N_p$  do
    Update parameters:
       $\Phi^{(i)} \sim \mathcal{N}(\Phi | \mathbf{m}_{t-1}^{i(j)}, h^2 V_{t-1})$ 
    Draw  $\theta_t^{(i)} \sim p(\theta_t | \theta_{t-1}^{i(j)}, \Phi^{(i)})$ 
    Calculate  $\tilde{w}_t^{(i)} = \frac{p(y_t | \theta_t^{(i)}, \Phi^{(i)})}{p(y_t | \mu_t^{i(j)}, \mathbf{m}_{t-1}^{i(j)})}$ 
  end for
  Normalise weights:  $w_t^{(i)} = \frac{\tilde{w}_t^{(i)}}{\sum_{i=1}^{N_p} \tilde{w}_t^{(i)}}$ 
end for

```

Algorithm 7 Storvik

```
1: initialisation;
2: for  $t \leftarrow 1$  to  $k$  do
3:   for  $i \leftarrow 1$  to  $N_p$  do
4:     Sample  $\Phi_t^{(i)} \sim p\left(\Phi | s_t^{(i)}\right)$ 
5:     Sample  $\tilde{\theta}_t^{(i)} \sim p\left(\theta_t | \theta_{0:t-1}^{(i)}, y_t, \Phi^{(i)}\right)$ 
6:     Calculate weights:
        
$$\tilde{w}_t \propto p\left(y_t | \theta_t^{(i)}, \Phi_t^{(i)}\right)$$

7:   end for
8:   Normalise weights:  $w_t^{(i)} = \frac{\tilde{w}_t^{(i)}}{\sum_{i=1}^{N_p} \tilde{w}_t^{(i)}}$ 
9:   Resample  $\left\{\theta_t^{(i)}, \Phi_t^{(i)}, s_t^{(i)}\right\}_{i=1}^{N_p}$  according
    to  $p(j(i) = l) = w_t$  (as discussed in Section 2.3)
10:  for  $i \leftarrow 1$  to  $N_p$  do
11:    Update sufficient statistics
        
$$s_t^{(i)} = \mathcal{S}\left(s_{t-1}^{(i(j))}, \theta_t, \theta_{t-1}, y_t\right)$$

12:  end for
13: end for
```

Algorithm 8 Particle Learning

```
1: initialisation;
2: for  $t \leftarrow 1$  to  $k$  do
3:   for  $i \leftarrow 1$  to  $N_p$  do
4:     Calculate  $\mu_t^{(i)} | \theta_t^{(i)}, s_t^{(i)}, \Phi_t^{(i)}$ 
5:     Calculate  $\tilde{w}_t^{(i)} \propto p\left(y_{t+1} | \mu_t^{(i)}\right)$ 
6:   end for
7:   Normalise weights:  $w_t^{(i)} = \frac{\tilde{w}_t^{(i)}}{\sum_{i=1}^{N_p} \tilde{w}_t^{(i)}}$ 
8:   Resample according to  $p(j(i) = l) = w_t$ 
9:   for  $i \leftarrow 1$  to  $N_p$  do
10:    Draw  $\theta_{t+1}^{(i)} \sim p\left(\theta_{t+1} | \mu_t^{(i)}, y_{t+1}\right)$ 
11:    Update the sufficient statistics
        
$$s_{t+1}^{(i)} = \mathcal{S}\left(s_t^{(i(j))}, \theta_{t+1}, \theta_t, y_{t+1}\right)$$

12:    Draw  $\Phi_{t+1}^{(i)} \sim p\left(\Phi_{t+1} | s_{t+1}^{(i)}\right)$ 
13:    Calculate  $\tilde{w}_t^{(i)} = \frac{p(y_{t+1} | \theta_{t+1}^{(i)})}{p(y_{t+1} | \mu_{t+1}^{(j)})}$ 
14:   end for
15:   Normalise weights:  $w_t^{(i)} = \frac{\tilde{w}_t^{(i)}}{\sum_{i=1}^{N_p} \tilde{w}_t^{(i)}}$ 
16: end for
```

B One step-ahead forecast

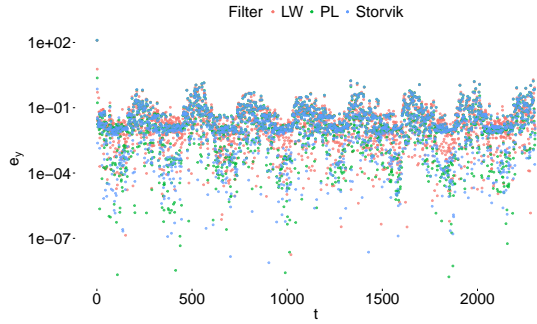


Figure B.1: Temperature data one-step ahead observation forecast errors.

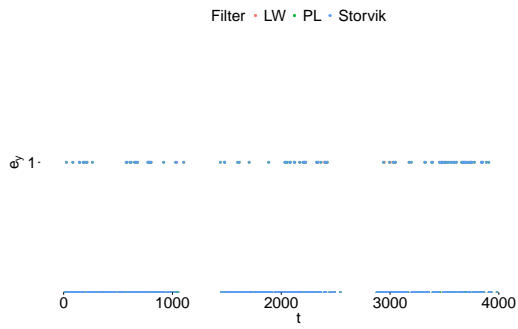


Figure B.2: Airport data one-step ahead observation forecast errors.

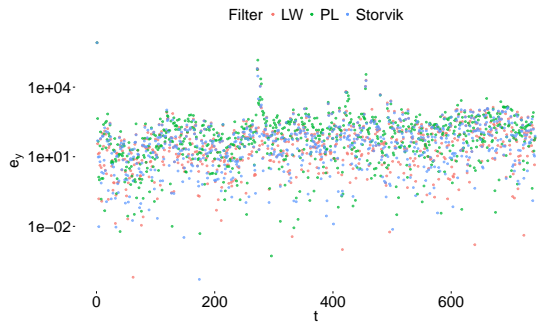


Figure B.3: WC98 data one-step ahead observation forecast errors.

C State forecast

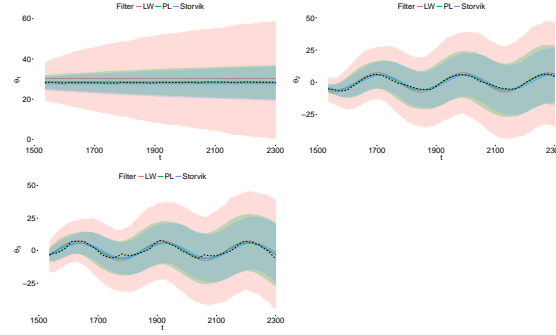


Figure C.1: State forecast for the temperature data

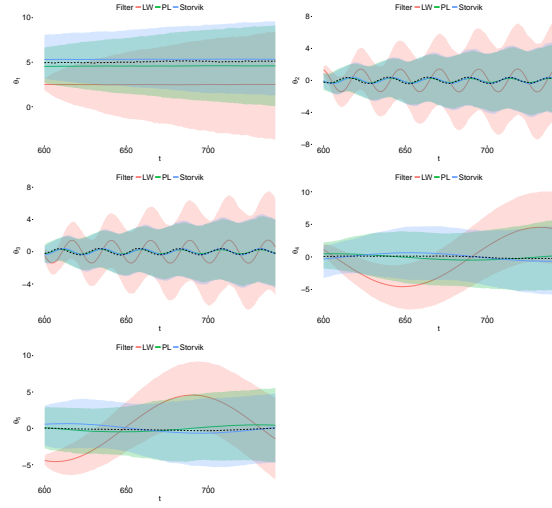


Figure C.3: State forecast for the WC98 data

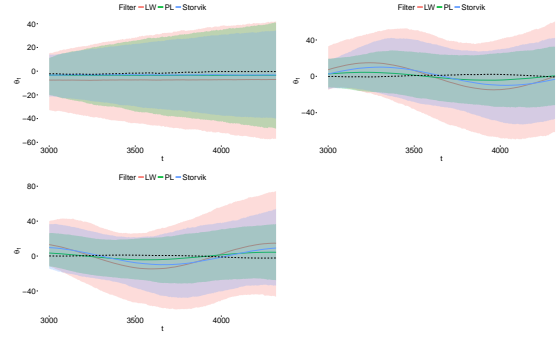


Figure C.2: State forecast for the airport data

D Execution time

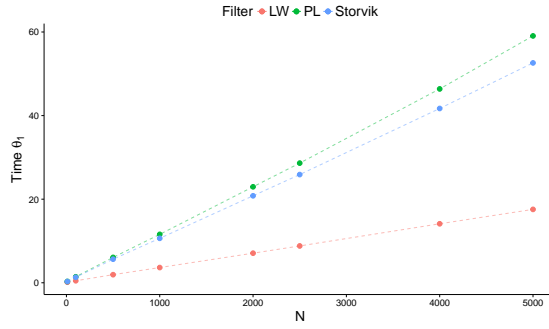


Figure D.1: LW, Storvik and PL execution time (seconds) for the temperature dataset using a Normal DLM with a varying number of particles.

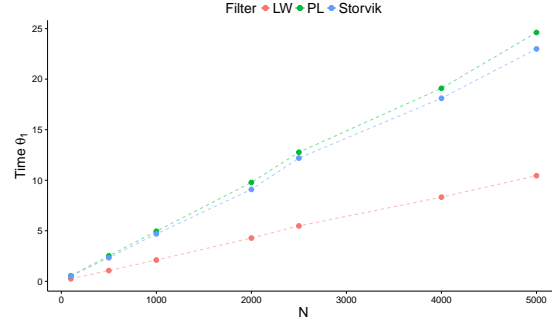


Figure D.3: LW, Storvik and PL execution time (seconds) for the WC98 dataset using a Poisson DLM with a varying number of particles.

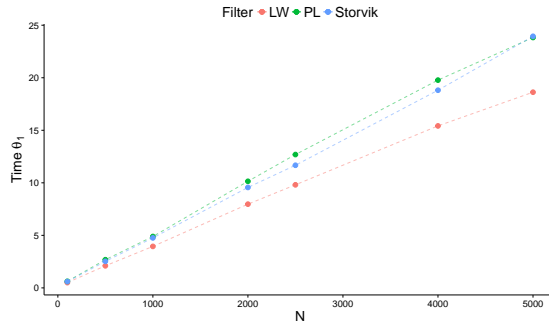


Figure D.2: LW, Storvik and PL execution time (seconds) for the airport dataset using a Binomial DLM with a varying number of particles.